

CHAPTER-VI

***High Temperature Ferroelectric
Phase Transition in BF-0.2PFN: A
Neutron Powder Diffraction Study***

6.1 Neutron powder diffraction study

In the previous chapter, we have unambiguously proved the absence of any intermediate β phase during R3c to $\text{Pm}\bar{3}\text{m}$ transition using laboratory source x-ray powder diffraction data. It was shown that high temperature cubic ($\text{Pm}\bar{3}\text{m}$) phase directly transformed into room temperature ' α ' phase through a coexistence region of R3c & $\text{Pm}\bar{3}\text{m}$ phases. However, using XRD data it was not easy to establish unambiguously whether the cubic phase transform directly into rhombohedral structure with R3c space group or via an intermediate rhombohedral structure with R3m space group. The ferroelectric distortion in both R3m and R3c space groups is revealed through identical characteristic splitting of the powder diffraction peaks whereas the presence of anti-phase tilted oxygen octahedra in R3c space group is distinguishable from the absence of such tilts in the R3m space group by the appearance of superlattice peaks having odd-odd-odd (ooo) indices with respect to a doubled pseudo cubic cell [Glazer (1975)]. Since the intensities of these superlattice peaks depend on small changes in the oxygen positions only, x-ray diffraction techniques are inadequate especially when the tilt angles are rather small in locating the oxygen positions accurately. Neutron diffraction is better suited for locating the small changes in the oxygen positions due to the antiferrodistortive phase transition in BF-xPFN leading to tilted oxygen octahedra. Therefore, we collected high resolution neutron powder diffraction (PND) data on BF-0.20PFN across the antiferrodistortive phase transition temperature to capture the superlattice reflections. The Rietveld refinement was also carried out for quantitative analysis of the neutron powder diffraction data.

6.2 Experimental

The neutron powder diffraction data were collected in the temperature range 650-1100 K using high-resolution powder diffractometer SPODI at FRM-II, Germany [Hoelzel et al. (2007)] at an incident neutron wavelength of 1.5483 Å using Nb sample holder. Approximately 20g of the sample was contained in a cylindrical niobium (Nb) holder with 50 μm wall thickness, 40mm height, and 10mm diameter for high temperature measurements in the vacuum furnace. The data were recorded at a step of 0.05° in the 2θ range of 5° to 130°.

6.3 Evolution of neutron powder diffraction patterns of BF-0.2PFN with temperature

Fig. 6.1 depicts the evolution of the 311_{pc}, 440_{pc}, 640_{pc} and 642_{pc} peak profiles in the temperature range 650-1025 K well above the magnetic transition temperature (T_N). At room temperature 311_{pc} superlattice peak has contribution from the antiferromagnetic ordering and antiphase rotation of the oxygen octahedra [Singh et al. (2011A)]. However, above magnetic transition temperature (T_N), entire contribution in intensity of 311_{pc} superlattice reflection is due to the antiphase rotation of oxygen octahedra. Intensity of 311_{pc} superlattice peak gradually decreases with increasing temperature in the temperature range 650 K ≤ T ≤ 850 K and sharply decreases at 900 K. However, very small intensity of superlattice reflection persists in the temperature range 900 K ≤ T < 950 K which can be clearly seen in the zoomed peaks above the area enclosed by the ellipses (see Fig. 6.1 (a)).

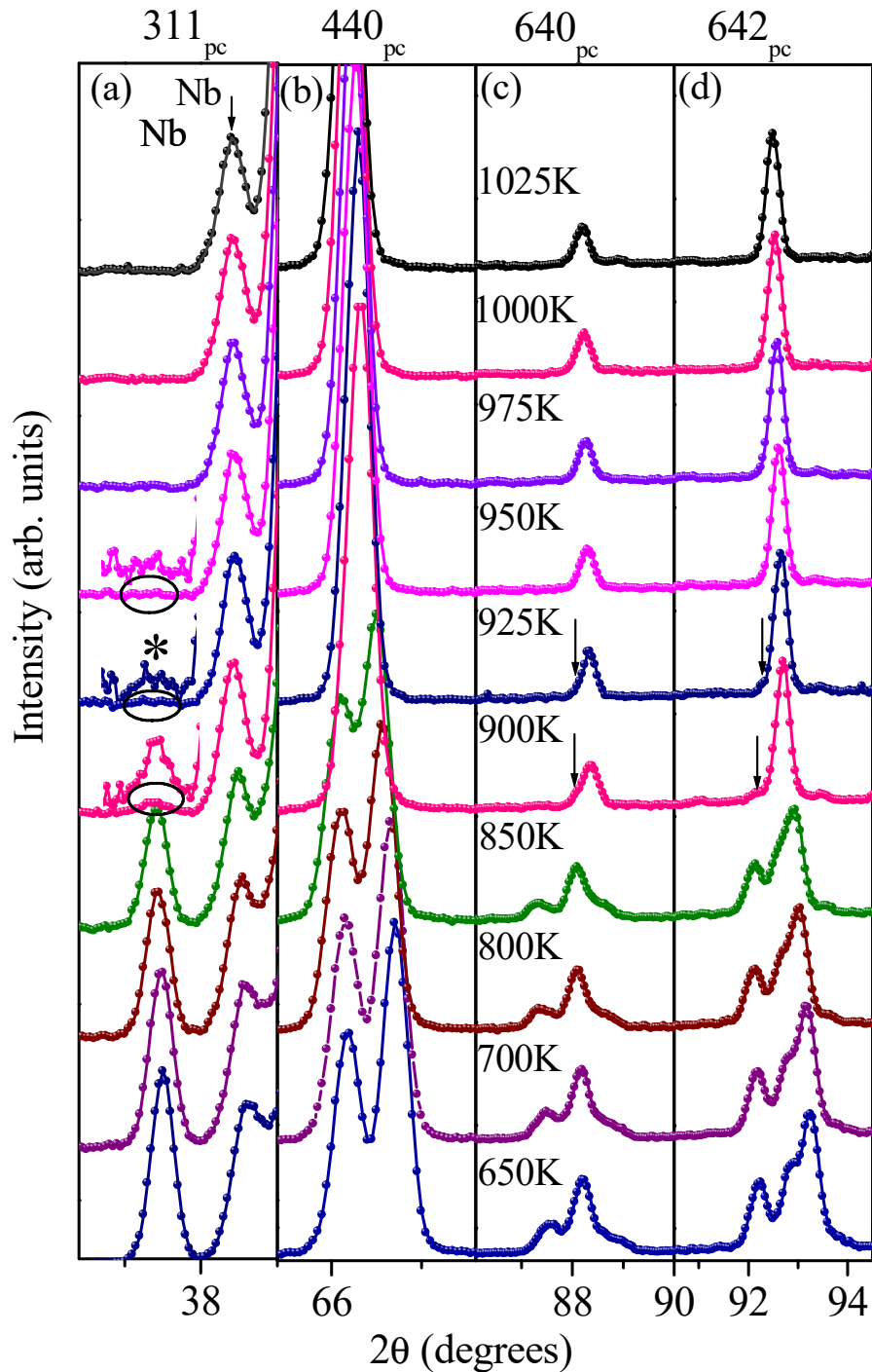


Fig. 6.1 Evolution of the Neutron powder diffraction data profiles for the pseudocubic (a) 311_{pc} (b) 440_{pc} (c) 640_{pc} and (d) 642_{pc} reflections with temperature. Asterisks in (a) indicate the super lattice reflection while the arrow indicates reflections due to the niobium sample holder. Arrows in (c) and (d) at left side of the main perovskite peak indicate reflection due to the R3c phase at 900 K and 925 K. Peak profile above the ellipses are the zoomed peak profile enclosed by respective ellipses.

Fig. 6.2 depicts the variation of integrated intensity of the 311_{pc} super lattice peak as a function of temperature. The least square fitted curve shown by solid line cuts the temperature axis at $T_{AFD} \sim 900$ K which gives an antiferrodistortive (AFD) phase transition temperature.

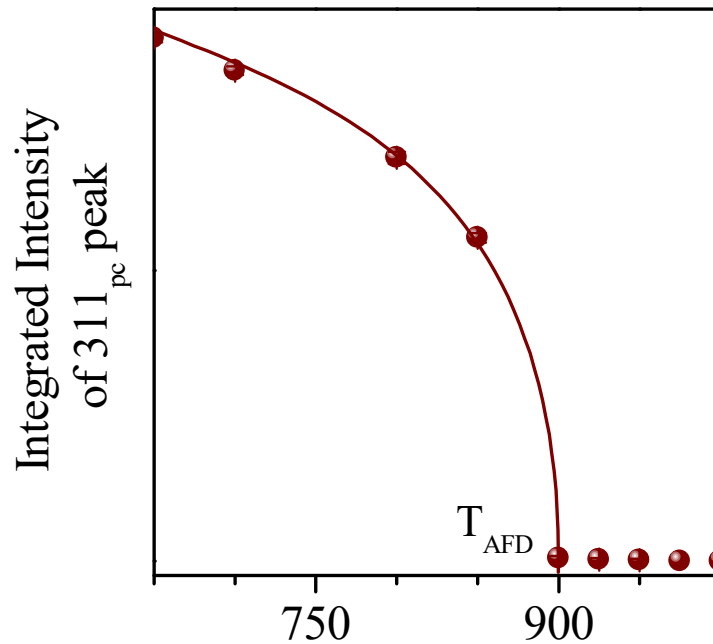


Fig. 6.2 Temperature dependent variation of integrated intensity of the 311_{pc} superlattice reflection in the temperature ranges $650 \leq T \leq 1000$ K.

The reflection marked by arrow in Fig. 6.1(a) is due to niobium (Nb) sample holder which was used at the time of data collection. The 440_{pc} peak, which is doublet for the $R3c$ space group, appears like a singlet at $T \geq 900$ K around the AFD phase transition temperature. Fig. 6.3 depicts the FWHM (full width at half maximum) plot of the 440_{pc} reflection for $T \geq 900$ K. The FWHM of the 440_{pc} reflection decreases abruptly and becomes constant only above $T \geq 950$ K. This means that large broadening of so-called “singlet peak” is due to the overlapping of more than one peak below $T < 950$ K. Above $T \geq 950$ K all the reflections are

singlet which is the characteristics of cubic ‘ γ ’ phase. The peak profiles 640_{pc} and 642_{pc} consist of four reflections for the R3c space group three of which can be seen from Fig. 6.1(c & d). All the three peaks start merging into a single peak with increasing temperature and seems to be singlet above $T \geq 900$ K with a small peak at tail end on the left-hand side of the 640_{pc} and 642_{pc} reflections (as shown by arrow in the Fig. 6.1(c & d) for the temperature range $900 \text{ K} \leq T < 950$ K. The peaks positions of the rhombohedral phase at $T \leq 850$ K match with the peaks positions of the reflections indicated by arrows in the Fig.6.1(c & d) in the temperature range $900 \text{ K} \leq T < 950$ K indicates the R3c phase persists into two phase region and completely disappear at $T \geq 950$ K.

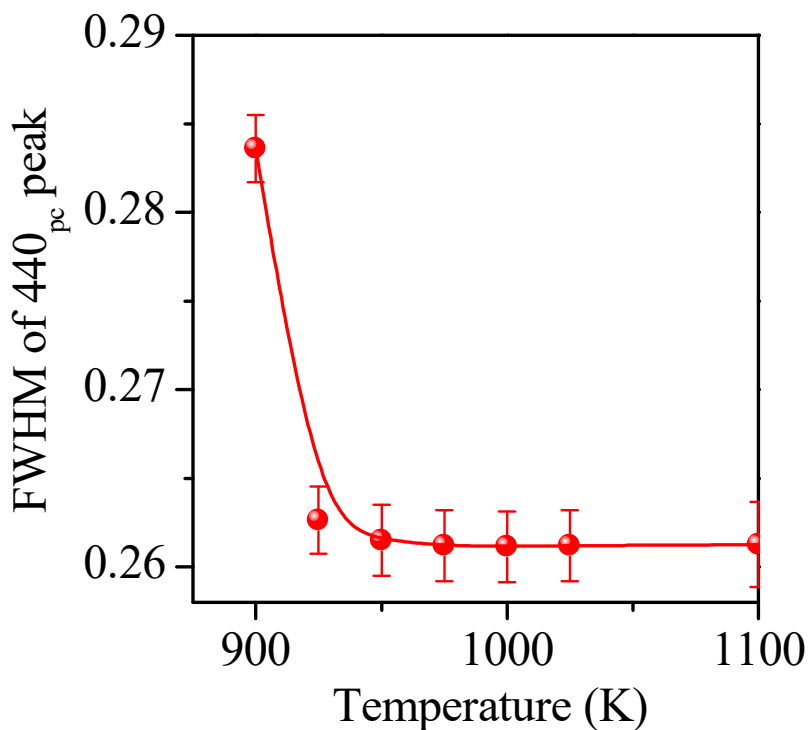


Fig. 6.3 The variation of FWHM of 440_{pc} profile as a function of temperature.

The reflections of both phases (high temperature paraelectric and low temperature ferroelectric) in the temperature range $900 \text{ K} \leq T < 950 \text{ K}$ are likely due to the co-existence of cubic and rhombohedral phases, which is the characteristic of first order ferroelectric to paraelectric phase transitions. The neutron powder diffraction profile shown in Fig. 6.1 reveals the presence of the 311_{pc} superlattice reflection in the temperature range $900 \text{ K} \leq T < 950 \text{ K}$, which rules out the possibility of an intermediate ‘ β ’ phase with $R3m$ space group.

6.4 Rietveld analysis of the neutron powder diffraction pattern

In order to confirm the above-mentioned qualitative observations, the neutron powder diffraction patterns were analyzed by the Rietveld refinement technique using FULLPROF package [Carvajal et al. (2010)]. Fig. 6.4 shows the observed, calculated, and difference profiles at 850 K (well above the magnetic transition temperature) in the 2θ range 10° - 150° using the $R3c$ space group. The inset of the same figure shows the fit profiles of 440_{pc} , 640_{pc} and 642_{pc} reflections in the zoomed scale. The fit between the observed and calculated profiles is quite good confirming the existence of $R3c$ phase well above the magnetic transition temperature. Results of a similar refinement using the neutron powder diffraction data at 900 K shown in Fig. 6.5 reveals rather poor fit.

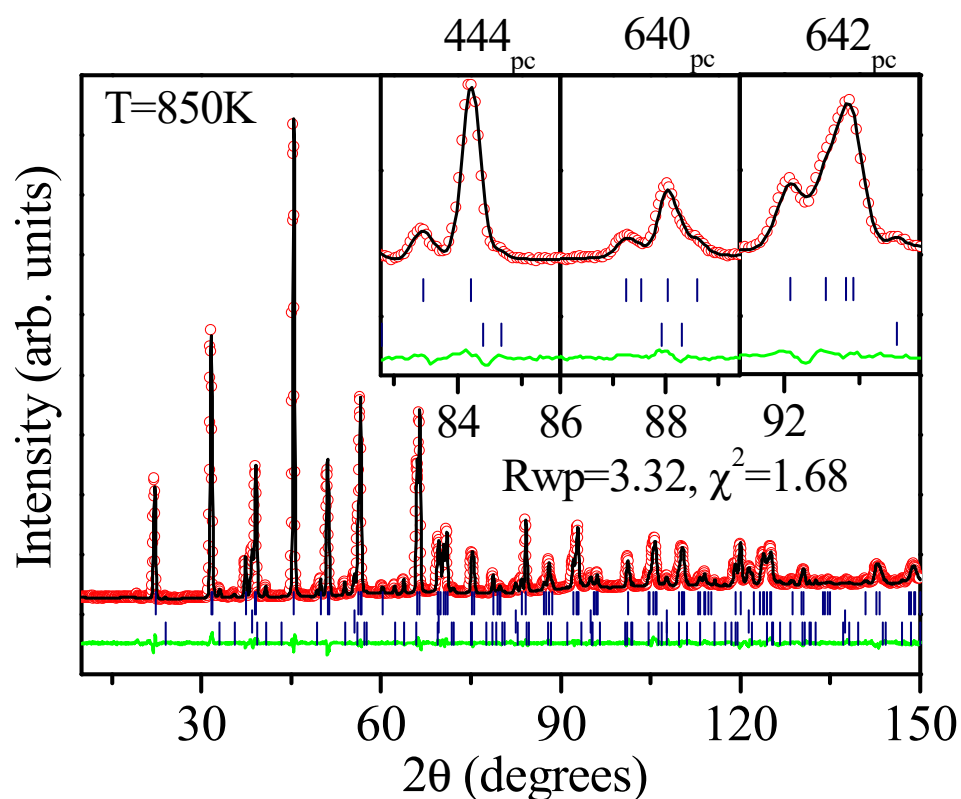


Fig. 6.4 Observed (circles), calculated (continuous line), and difference (bottom line) patterns obtained after the Rietveld refinement of neutron powder diffraction data at $T = 850\text{ K}$ using $R3c$ space group. Insets show zoomed portion of the Rietveld fit for the 444_{pc} , 640_{pc} and 642_{pc} peak profiles. The upper tick marks indicate the nuclear peaks due to the $R3c$ phase while the lowest tick marks indicate the peaks due to small trace of the Fe_2O_3 . The middle tick marks are due to the niobium sample holder.

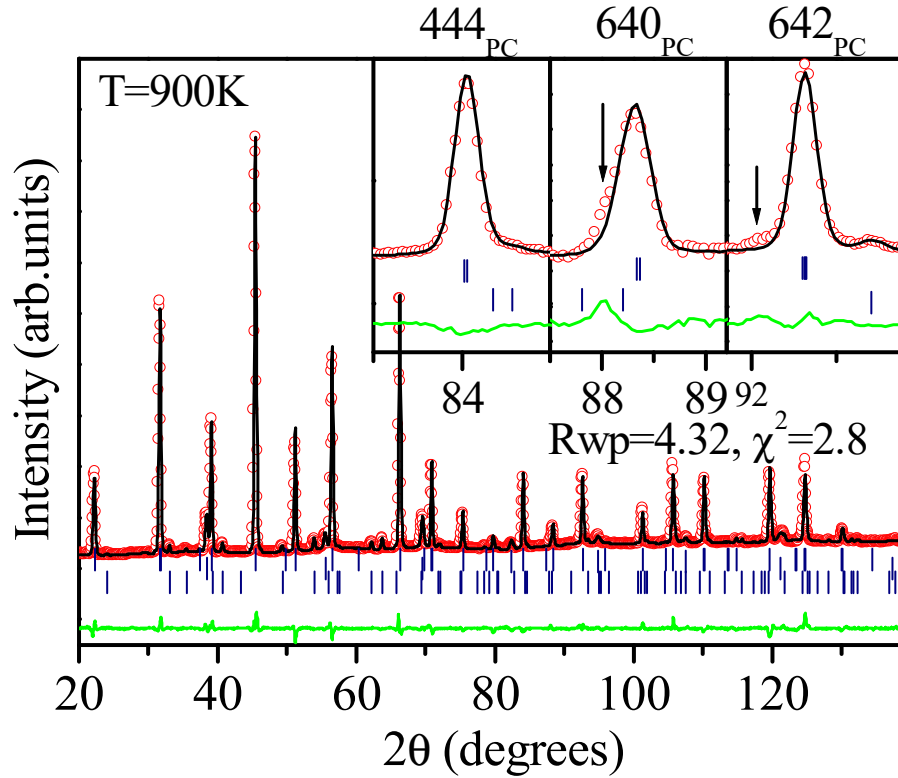


Fig. 6.5 Observed (circles), calculated (continuous line), and difference (bottom line) patterns obtained after the Rietveld refinement of neutron powder diffraction data at $T = 900$ K using R3c space group. The upper tick marks indicate nuclear peaks due to the R3c phase while lowest tick marks indicate peaks due to small trace of the Fe_2O_3 . The middle tick marks are due to niobium sample holder. Insets show zoomed portion of the Rietveld refinement fit of the 444_{pc} , 640_{pc} and 642_{pc} peak profiles. The arrows in insets indicate mismatch between observed and calculated profiles.

In particular, the peak positions marked with arrows on the left-hand side of the 640_{pc} and 642_{pc} profiles are not properly accounted for using the R3c space group. It also gives higher values for the $R_{\text{wp}} \sim 4.32$ and $\chi^2 \sim 2.8$ in comparison to the refinement fit at 850 K. Our previous XRD studies have revealed that in the

temperature range 873-973 K, the rhombohedral phase co-exists with the cubic paraelectric phase as a result of first-order character of the $R3c$ to $Pm\bar{3}m$ phase transition.

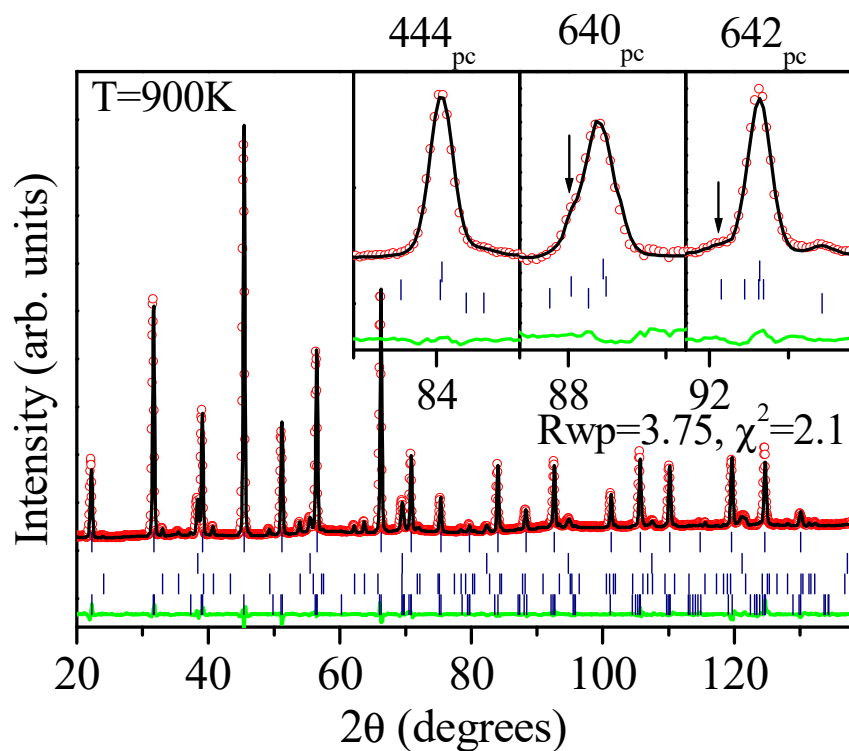


Fig. 6.6 Observed (circles), calculated (continuous line), and difference (bottom line) patterns obtained after the Rietveld refinement of neutron powder diffraction data at $T = 900$ K using $R3c+Pm\bar{3}m$ space groups. The upper most and lower most tick marks indicate nuclear peaks due to $Pm\bar{3}m$ and $R3c$ phase respectively while second and third tick marks below observed and calculated profiles are due to the Nb-sample holder and small trace of Fe_2O_3 respectively. Insets show zoomed portion of the Rietveld refinement fit of 444_{pc} , 640_{pc} and 642_{pc} peak profiles.

The qualitative analysis of neutron powder diffraction data also signals the coexistence of two phases in the temperature range $950 < T < 950$ K. We therefore considered co-existence of rhombohedral R3c and cubic $Pm\bar{3}m$ phases for the Rietveld refinement in this temperature range. The Rietveld fit at $T = 900$ K is shown in Fig. 6.6.

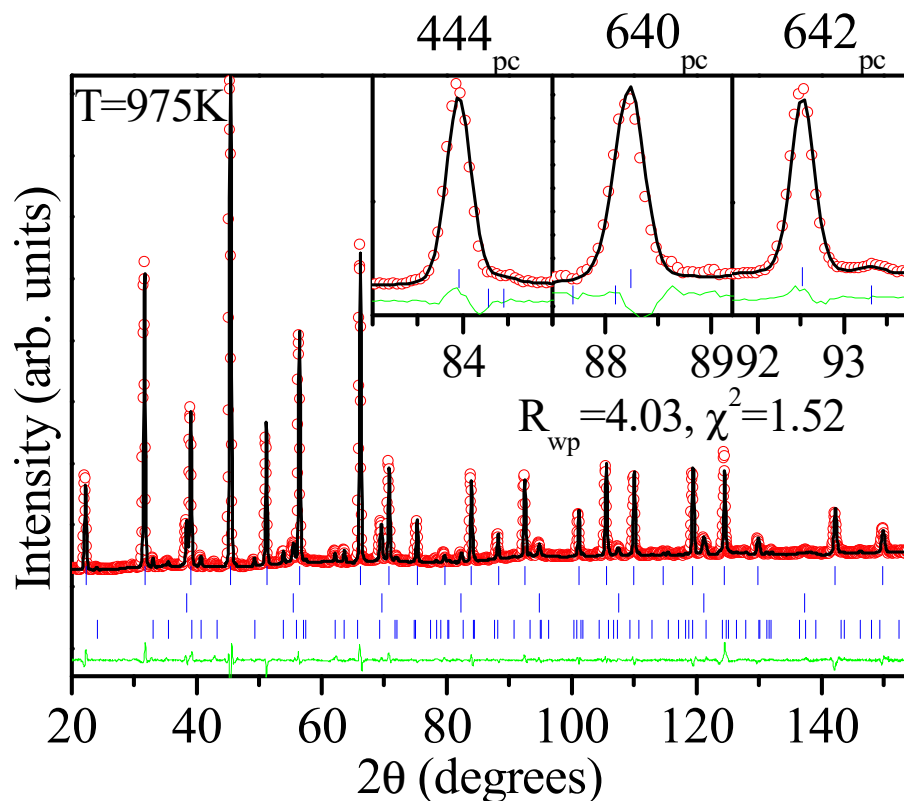


Fig. 6.7 Observed (circles), calculated (continuous line), and difference (bottom line) patterns obtained after the Rietveld refinement of the neutron powder diffraction data at $T = 975$ K by using $Pm\bar{3}m$ space group. The upper tick marks indicate the nuclear peaks due to the $Pm\bar{3}m$ phase while lowest tick marks indicate the peaks due to small trace of the Fe_2O_3 . The middle tick marks are due to the niobium sample holder. Insets show zoomed portion of the Rietveld fit of 444_{pc} , 640_{pc} and 642_{pc} peak profiles.

It is evident from this figure that two phases model $R3c+Pm\bar{3}m$ accounts all the peaks and also gives very good overall fit. All the reflections of the neutron powder diffraction data collected above $T \geq 950$ K is singlet. Therefore, cubic model with $Pm\bar{3}m$ space group was used for the Rietveld refinement. Fig. 6.7 depicts the Rietveld fit for neutron powder diffraction data collected at $T = 975$ K. The fit between the observed and calculated profiles is quite good confirming the existence of cubic phase with $Pm\bar{3}m$ space group above $T \geq 950$ K.

6.5 Unit cell parameters, Polarization and Tilt angle

Figure 6.8 (a) depicts the variation of lattice parameters and unit cell volume as a function of temperature in the temperature range 650-1100 K obtained from the Rietveld refinements. A discontinuous change in the unit cell volume ($\Delta V \sim 0.20 \text{ \AA}^3$ at 900 K) at the rhombohedral to cubic phase transition confirms the first order character of the $R3c$ to $Pm\bar{3}m$ phase transition. The order parameters associated with the ferroelectric and AFD phase transitions are polarization and octahedral tilt angle respectively. Polarization in the temperature range 650-1100 K is calculated by using the formula: $P = (e/V) \sum_k z_k' \Delta(k)$, where $\Delta(k)$ is the displacement of the k th ion from its ideal cubic perovskite position, z_k' is the Born effective charges for the k th ion and V is the volume of the primitive unit cell, while the sum runs over all the ions inside the unit cell which will also be discussed in chapter VIII.

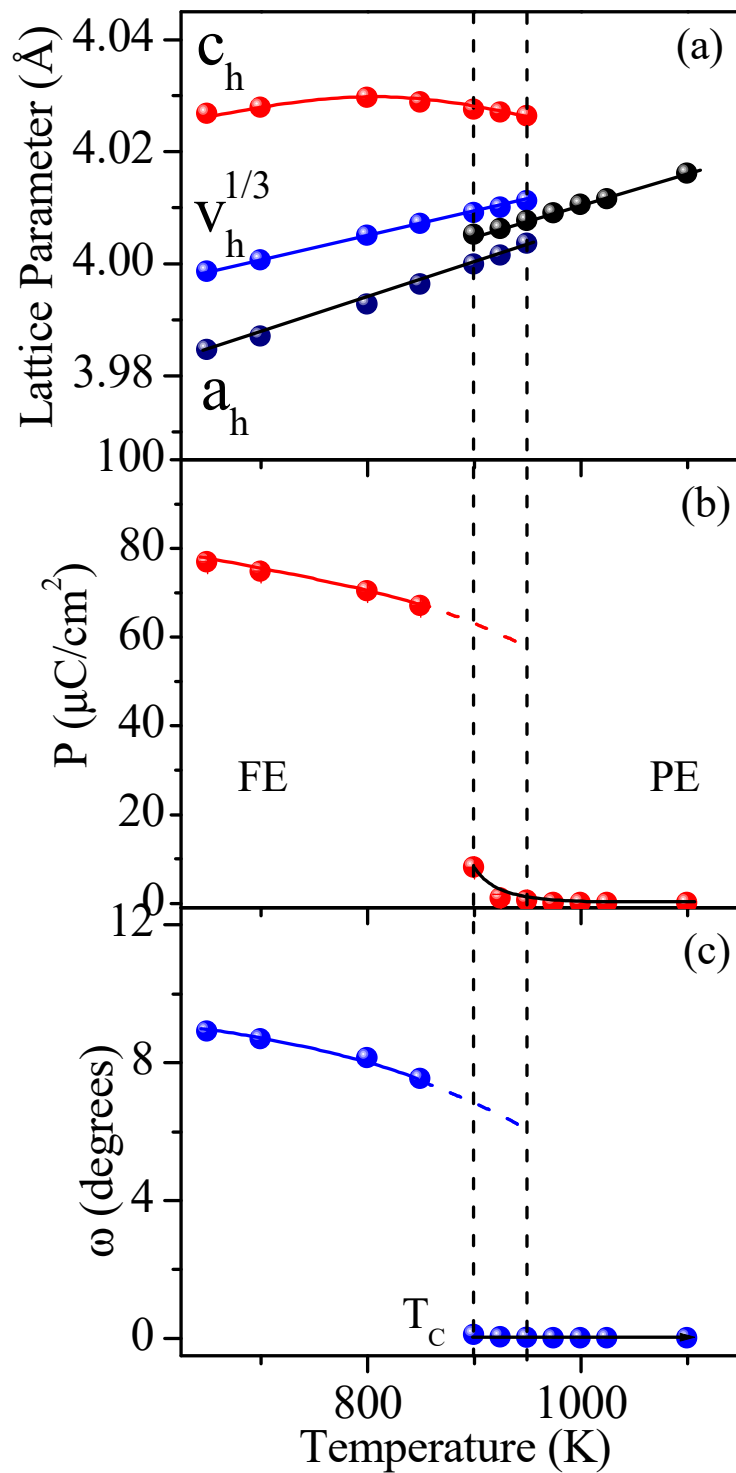


Fig. 6.8 Variation of (a) pseudocubic cell parameters and unit cell volume (b) calculated ionic polarization (P) along the $[111]$ directions of the pseudocubic cell (c) tilt angle (ω) of the antiphase rotation of oxygen octahedra about the $[111]$ direction as a function of temperature in the temperature range 650-1100 K.

Fig. 6.8(b) depicts the variation of the ionic polarization with temperature. The calculated polarization (P) gradually decreases with increasing temperature until it vanishes discontinuously at $T \geq 900$ K in the paraelectric phase. We have calculated tilt angle ω using ‘e’ parameter obtained from the Rietveld refinement positional coordinates and plotted it as a function of temperature. The calculated tilt angle (ω) gradually decreases with increasing temperature until it vanishes discontinuously at $T \geq 900$ K in the cubic phase [see Fig. 6.8(c)] further confirming first order character of this phase transition. The results presented in Fig. 6.8 evidently suggest that both the order parameters (tilt angle and polarization) emerge below the cubic to rhombohedral phase transition temperature simultaneously rather than successively. This implies that none of the two order parameters can be termed secondary, as both are equally important for the R3c phase to emerge from the $Pm\bar{3}m$ phase. Thus the $Pm\bar{3}m$ to R3c phase transition is an unusual type of phase transition for which no one single primary order parameter can be defined. On the contrary, this transition results from the cooperation of two primary order parameters. In literature, this kind of transition has been termed as a “Trigger type transition”. We thus conclude that the R3c to $Pm\bar{3}m$ transition in BF-0.2PFN solid solution is of trigger type phase transition [Holakovsky (1973)].

6.6 Summary and conclusions

The results of the high temperature neutron powder diffraction study on the BF-0.2PFN solid solution can be summarized as follows:

(i) The R3c phase of BF-0.2PFN transform directly into ‘ γ ’ phase without any intermediate β -phase. The presence of 311_{pc} type of superlattice reflections across two phase region excludes the possibility of R3m phase as one of the intermediate β -phase.

(ii) The existence of phase coexistence in the temperature range $850 < T < 950$ along with significant jump in the unit cell volume at ferroelectric to paraelectric phase transition temperature confirms first order character of ferroelectric to paraelectric phase transitions in BF-0.2PFN solid solutions.

(iii) The simultaneous appearance of the polarization and tilt order parameters below the paraelectric to ferroelectric phase transition is indicate of an unusual “trigger type” of phase transitions where two order parameters emerge simultaneously, none of which is secondary to the other.

(iv) The results obtained by high temperature neutron powder diffraction study on the BF-0.2PFN samples supports our previous investigation based on laboratory source x-ray powder diffraction study.